The 9th Asian-Pacific Congress for Parasitic Zoonoses, Gifu, Aug. 2006

6）Yoshida T, Arai T, Nakamoto K, Iseki M, Tokoro M
Are humans the only host for *Cyclospora cayetanensis* ? : A gene analysis to detect zoonoses
The 9th Asian-Pacific Congress for Parasitic Zoonoses, Gifu, Aug. 2006

7）仲本　賢太郎、所　正治
腸管寄生原虫のPCRによる検出
第24回北陸病害動物研究会（2006.5、富山）

8）山口智博, 及川陽三郎, 所　正治
ジアルジア（ランブル鞭毛虫）の遺伝子型解析
第24回北陸病害動物研究会（2006.5、富山）

9）荒井朋子, 吉田知代, 古川博, 小松八千代, 所　正治
PCR法によるサイクロスポーラの検出
第24回北陸病害動物研究会（2006.5、富山）

１０）所　正治、古川　博、小松八千代、吉田知代、荒井朋子、井関基弘
PCR法によるサイクロスポーラの検出
第１７回日本臨床寄生虫学会（2006.6、東京）

１１）仲本賢太郎、坪井敬文、所　正治、野崎知義
赤痢アメーバにおけるS-adenosyl-L-methionine synthaseおよびS-adenosyl-L-homocysteine hydrolaseの解析
第７５回日本寄生虫学会大会（2006.5、弘前）

１２）所　正治、仲本賢太郎、荒井朋子、井関基弘
ジアルジアの遺伝子型における多型解析
第７５回日本寄生虫学会大会（2006.5、弘前）

１３）原田倫世、藤本陽子、中村公亮、城戸康年、坂本君平、八木欣平、所　正治、藪義貞、鈴木高史、北潔
Cryptosporidiumシアン耐性酸化酵素（AOX）の解析
第７５回日本寄生虫学会大会（2006.5、弘前）

１４）荒井朋子、仲本賢太郎、木俣勲、北出幸夫、坪井敬文、所　正治
リアルタイムPCRを用いたアデノシンアナログのクリプトスポリジウム増殖抑制効果の評価
第７５回日本寄生虫学会大会（2006.5、弘前）

１５）中村一内山ふくみ、所　正治、福田一、鮫島直樹、澤田浩武、布井博幸、廣松賢治、名和行文
治療に難渋した無γ－グロブリン血症患者のランブル鞭毛虫症の１例
第７５回日本寄生虫学会大会（2006.5、弘前）

G.　知的所有権の取得状況

１．特許取得
該当せず。

２．実用新案登録
該当せず。

厚生労働科学研究費補助金（新興・再興感染症研究事業）
分担研究報告書

施設内原虫感染等の疫学的解析；施設内感染介入策作成と感染抑止の関連解析；感染株の分離・維持

分担研究者　鈴木　淳　　東京都健康安全研究センター微生物部病原細菌研究科

研究要旨　1）赤痢アメーバ施設内集団感染の実態調査：2005年度に調査を終了した東京都知的障害者更生施設4施設に加え，2006年3月より新たに同じ東京都および近県の施設について，知的障害者更生施設4施設，327名（男性240名，女性87名）の糞便検査（顕微鏡検査，赤痢アメーバ抗原検出検査）が終了した。いずれの施設からも赤痢アメーバ感染者は検出されなかったが，1施設の1生活棟において*Entamoeba dispar*への感染が3名に認められた。また、本調査に用いた赤痢アメーバ抗原検出キット（*E. histolytica*Ⅱ）の1ロットに擬陽性を示す場合があることを確認した。
2）東京都定点医療機関受診者（女性）の赤痢アメーバ抗体保有率調査：2006年の赤痢アメーバ抗体陽性率は5.3%であった。また，2003年から2005年の抗体陽性率が，それぞれ1.5%，3.7%，5.0%と抗体保有率に上昇傾向が見られ，ヘテロセクシュアル間の性行為を通して感染する女性の赤痢アメーバ感染者数が増加していることが示唆された。

A. 研究目的

1）施設内腸管寄生原虫の感染実態調査：

下痢症の原因となる腸管寄生性原虫のヒトへの感染は，主に無症状感染者の糞便中に排出される感染型原虫（シストまたはオーシスト）を手指や飲食物を介して経口摂取することにより成立する。そのため，適切な糞便の処理や手洗いによりその感染防止が可能であるが，自ら感染防止対策を行うことが困難な人が利用する施設においては，感染者の存在が施設内での集団下痢症につながることが危惧される。そこで，知的障害者施設における赤痢アメーバ等の腸管寄生原虫の感染実態調査を行い，その結果をもとに赤痢アメーバ症のより効果的な予防と防御対策を立案する。そしてこれらの対策を実施，評価，改良し，他施設へ還元すること及び今後の厚生・福祉行政へ反映させることを目的とする。

2）赤痢アメーバ抗体保有率調査：近年、赤痢アメーバ症の報告数で女性の患者報告者数が増加の兆しを見せている。そこで、ヘテロセクシュアル間の性行為感染症としての赤痢アメーバの感染実態の把握を目的に，東京都定点医療機関受診者の女性における赤痢アメーバ抗体保有状況を調査し、赤痢アメーバ感染蔓延防止策の基礎資料とすることを目的とする。

B. 研究方法

1）赤痢アメーバ等の腸管寄生原虫の施設内感染状況の実態調査：東京都の知的障害者更生施設を対象として新たに2006年3月から東京都健康安全研究センターにより調査が開始され，4施設，327名の糞便検査（顕微

鏡検査，赤痢アメーバ抗原検出，PCR 法による遺伝子診断）を実施した。また，1 施設においては，赤痢アメーバの感染の疑いが認められたことから，赤痢アメーバ抗体検査も実施した。

2）東京都感染症サーベイランス事業における東京都定点医療機関（1 箇所）の協力を得て，受診者（女性）を対象とした血清学的に赤痢アメーバ抗体保有率の調査を行った。検査方法は赤痢アメーバ無菌培養株(HM-1:IMSS,c16)を抗原として，プレート ELISA（IgG）法により行った。

C. 研究結果

1）今回，感染実態調査を行った 4 施設（K, L, M, N），327 名について，ホルマリン・エーテル法による顕微鏡検査，*E. histolytica*Ⅱキットを用いた赤痢アメーバ特異抗原検出検査及び PCR 法を用いた赤痢アメーバの遺伝子検出検査を行った結果，4 施設いずれからも赤痢アメーバは認められなかった。しかし，PCR 法を用いた確認検査により，1 施設(N)において病原性はないが形態学的に赤痢アメーバに酷似した *Entaomeba dispar* の感染が 3 名に認められた。また、無菌培養に成功した 2 株のアイソエンザイムパターンは、共にザイモデム I 型であった。また，赤痢アメーバと同一の感染経路をとると考えられる非病原性の大腸アメーバ，小形アメーバの感染が 3 施設(L, M, N)，計 24 名(施設 L：1/59，施設 M：1/44，施設 N：22/150)から検出された。*E. dispar* が見とれられた施設において大腸アメーバ，小形アメーバの感染が認められた利用者は同一の生活棟であると報告された。また，*E. dispar* の感染が認められた施設 N 利用者は 3 例共に 20 歳代男性であったが，大腸アメーバ，小形アメーバの感染が認められた施設利用者の年齢は 20 歳代から 60 歳代と様々な年代で感染が認められた。

今回の調査において赤痢アメーバ抗原検出検査（*E. histolytica*Ⅱキット）で陽性であったが，その後の複数回の検便検査及び赤痢アメーバ抗体検査で陰性を示す例が計 5 例（施設 K：2 例，施設 L：1 例，施設 N：2 例）に認められた。いずれも同一ロットを使用していたが，施設 N の 2 例について別ロットによる検査では陰性であったことから，*E. histolytica*Ⅱキットはロットにより偽陽性を示す場合があることが示唆された。

2）対象となった東京都定点医療機関における

2006 年の赤痢アメーバ抗体陽性率は 5.3%（15/285）であった。2003 年から 2004 年の抗体陽性率が，それぞれ 1.5%，3.7%，5.0%であったことから，さらなる抗体保有率に上昇傾向が見られた。また，年代別赤痢アメーバ抗体陽性者は，陽性例 15 件の年代は 20 歳代 9 例，30 歳代 3 例，40 歳代 2 例，50 歳代 1 例と比較的若い年代に陽性例が多く認められた。

D. 考察

1）2006 年度は新たに知的障害者更正施設の 4 施設（男性：240 名，女性：87 名）を対象とした調査により，*E. dispar* の施設内感染が確認された。また，*E. histolytica*Ⅱキットの使用でロットにより偽陽性を示すことが認められた。これらのことから，赤痢アメーバの検査においては，顕微鏡検査と PCR 法による遺伝子検査など複数の検査法を組み合わせて行うことが必要であると考えら

れた。また，同一の生活棟において *E. dispar*，大腸アメーバ等の感染が認められたことから，施設利用者の中に赤痢アメーバ等の腸管寄生原虫感染者がいた場合，他の施設利用者への感染拡大が危惧された。

2）定点医療機関受診者における女性の赤痢アメーバ抗体保有率調査では，2003 年からの 2006 年の 4 年間，赤痢アメーバ抗体保有率に上昇傾向も見られており，ヘテロセクシュアル間の性行為による感染する女性の赤痢アメーバ感染者数が増加していることが示唆された。

F. 健康危険情報　なし

G. 研究発表

1．　論文発表

1）Suzuki J, Kobayashi S, Murata R, Yanagawa Y, Takeuchi T. 2007. Profiles of a pathogenic *Entamoeba histolytica*-like variant with variations in the nucleotide sequence of the small subunit ribosomal RNA isolated from a primate (De Brazza's Guenon). Journal of Zoo and Wildlife Medicine. In press.

2）鈴木　淳，村田理恵，小林正規，柳川義勢，竹内　勤：知的障害者更正施設における赤痢アメーバ等腸管寄生原虫の感染実態調査(2)－*E. dispar* の施設内感染を中心にしてー，日本臨床寄生虫学会誌，17，52-55，2006.

2．　学会発表

1）鈴木　淳，村田理恵，小林正規，柳川義勢，竹内　勤：知的障害者更正施設における赤痢アメーバ等腸管寄生原虫の感染実態調査(2)－*E. dispar* の施設内感染を中心にしてー (2006)

H. 知的財産権の出願・登録状況

1. 特許取得　　なし
2. 実用新案登録　　なし
3. その他　　なし

GROWTH-PROMOTING EFFECT ON IRON-SULFUR PROTEINS ON AXENIC CULTURES OF *ENTAMOEBA DISPAR*

KHALIFA S.A.M.*, IMAI E.*, KOBAYASHI S.*, HAGHIGHI A.**, HAYAKAWA E.* & TAKEUCHI T.*

Summary:

A growth-promoting factor (GPF) that promotes the growth of *Entamoeba dispar* under axenic culture conditions was found in fractions of mitochondria (Mt), hydrogenosomes (Hg) and chloroplasts (Cp) obtained from cells of six different protozoan, mammalian and plant species. We were able to extract the GPF from the Cp-rich leaf cells of a plant (spiderwort: *Commelina communis* L.) in an acetone-soluble fraction as a complex of chlorophyll with low molecular weight proteins (molecular weight [MW] approximately 4,600). We also found that on treatment with 0.6 % complexes of 2-mercapthoethanol (2ME), complexes of chlorophyll-a with iron-sulphur (Fe-S) proteins (e.g., ferredoxins [Fd] from spinach and *Clostridium pasteurianum*) and noncomplex rubredoxin (Rd) from *C. pasteurianum* have a growth-promoting effect on *E. dispar*. These findings suggest that *E. dispar* may lack a sufficient quantity of some essential components of Fe-S proteins, such as Fe-S center.

KEY WORDS : growth, mitochondria, hydrogenosomes, chloroplasts, iron-sulphur protein, *Entamoeba dispar*.

Résumé : LES EFFETS D'ACCÉLÉRATION DE CROISSANCE DES PROTÉINES FER-SOUFRE DANS LA CULTURE AXÉNIQUE D'*ENTAMOEBA DISPAR*

*Des facteurs d'accélération de croissance (Growth promoting factor: GPF) favorisant le développement d'*Entamoeba dispar *ont été détectés dans la composition de la mitochondrie, de l'hydrogénosome et du chloroplaste isolés à partir de six sortes de cellules issues de protozoaires, mammifères et plantes. De plus, les GPF de cellules de mésophile contenant une grande quantité de chloroplaste végétal (*Commelina communis *L.) ont pu être extraits comme une substance composée de protéines de faible masse moléculaire (≈ 4 600) et de chloroplastes dans la composition acétone-soluble. À partir de ces résultats, nous avons préalablement pu découvrir des effets d'accélération de croissance dans le corps composé de protéines fer-soufre (épinard et ferrédoxine de* Clostridium pasteurianum*) et de chlorophylle-a traité au 2-mercaptoéthanol 0,6 % et du corps simple rubrédoxine de* C. pasteurianum. *Ces observations ont suggéré qu'une composante essentielle formant la protéine fer-soufre d'*E. dispar *(comme noyau fer-soufre) semblait être insuffisante.*

MOTS CLÉS : *croissance, mitochondrie, hydrogénosome, chloroplaste, protéine fer-soufre,* Entamoeba dispar.

INTRODUCTION

Entamoeba dispar grows well under xenic and monoxenic culture conditions along with enteric bacteria such as *Escherichia coli* or anaerobic bacteria such as *Fusobacterium symbiosum* (*Clostridium symbiosum* ATCC 14940) (Robinson, 1968; Diamond, 1982; Vargas *et al.*, 1990). However, even after the introduction of the axenic yeast extract-iron serum (YI-S) medium for *E. dispar* (Diamond *et al.*, 1995; Clark, 1995) the axenic cultivation of *E. dispar* remains difficult. Compared with *E. dispar*, pathogenic *E. histolytica*, which is closely related to *E. dispar*, easily adapts to the axenic culture medium (TYI-S-33) (Diamond *et al.*, 1978). Additionally, *Entamoeba histolytica* is capable of invading the mucosa of the large intestine. We have also developed a new yeast extract-iron-gluconic acid-dihydroxyacetone-serum medium (YIGADHA-S) (Kobayashi *et al.*, 2005) based on the YI-S medium and on the results of an investigation on bacterial metabolic products, and have succeeded in culturing five strains under axenic conditions. However, despite using the YIGADHA-S culture system, the axenic growth of four of five strains of *E. dispar* was found to be very poor, with the exception of one primate-derived strain (CYNO 09: TPC) isolated from a cynomolgus monkey. A further search for useful growth promoting factors (GPFs) revealed that autoclaved (121° C, 15 minutes) bacteria and more than 20 types of protozoan, mammalian and plant cells containing mitochondria (Mt), hydrogenosomes (Hg) and chloroplasts (Cp) have a significant growth-promoting effect on *E. dispar*. However, the degree of these growth-promoting effects differs among the GPFs. In the present study, we were able to extract GPF from the Cp-rich leaf cells of a plant (spiderwort: *Commelina communis* L.) in an acetone-soluble fraction as a chlorophyll complex with low mole-

* Department of Tropical Medicine and Parasitology, School of Medicine, Keio University, Shinjuku-ku, Tokyo, Japan.
** Department of Medical Parasitology and Mycology, School of Medicine Shaheed University of Medical Sciences, Eveen, Teheran 19395, Iran.
Correspondence: Seiki Kobayashi, PhD., Department of Tropical Medicine and Parasitology, School of Medicine, Keio University, 35 Shinanomachi, Shinjuku-ku, Tokyo 160-8582, Japan.
Tel.: +81-3-5363-3761 – Fax: +81-3-3353-5958.
E-mail: skobaya@sc.itc.keio.ac.jp

cular weight proteins. Significant amounts of iron (Fe), sulphur (S) and molybdenum (Mo) atoms were found in the protein-chlorophyll complex fraction along with the magnesium (Mg) atom of chlorophyll.

Based on these findings, we hypothesized that some common components of Fe-S proteins present in Mt, Hg, Cp and bacteria support the growth of *E. dispar*. This is because in *E. dispar*, an essential redox Fe-S protein [ferredoxin (Fd)] is expected to be involved in energy metabolism, such as oxidative decarboxylation of pyruvate to acetyl-coenzyme A (acetyl-CoA), which is similar to that found in *E. histolytica* (McLaughlin & Aley, 1985).

MATERIALS AND METHODS

E. DISPAR ISOLATE

In this study, one human-derived strain of axenically grown *E. dispar* (AS 16 IR) (Kobayashi *et al.*, 2005) was used to determine the growth promoting effect of Fe-S proteins.

AXENIC CULTIVATION OF *E. DISPAR*

The YIGADHA-S medium (Kobayashi *et al.*, 2005) containing 15 % heat-inactivated bovine serum was used as the axenic cultivation medium for *E. dispar*.

DONOR CELLS OF MT, HG, CP AND MITOSOMES

The Mt donors are as follows: protozoan parasites: i) *Crithidia fasciculata* (ReF-1, PRR strain, ATCC 50083); ii) *Trypanosoma cruzi* (Tulahuen strain); iii) *Leishmania major* (MHOM/SU/73/5-ASKH strain, ATCC 50155); and iv) *Acanthamoeba castellanii* (ATCC 30011). v) The vertebrate cells used as Mt donors were from the mouse lymphoblast cell line (P388D1, ATCC CCL-46). The Hg donors are as follows: protozoan parasites: vi) *Trichomonas vaginalis* (KO-11 strain) (Qi *et al.*, 1995) and vii) *Trichomonas foetus* (Okamoto *et al.*, 1998). viii) Leaves of the spiderwort (*Commelina communis* L.) were used as the Cp donors. Consisting amitochondrial protozoan parasite mitosomes that are mitochondrial remnant organelles (Tovar *et al.*, 2003) was used as the mitosome donor, ix) *Giardia intestinalis* (syn. *lamblia*), (Portland-I strain, ATCC 30888). The bacterium used was *Pseudomonas aeruginosa* (PA:KEIO strain) (Kobayashi *et al.*, 1998).

PREPARATION OF CELLS

C. fasciculata and *T. cruzi* were axenically cultured in liver infusion tryptose (LIT) medium (*Gutteridge et al.*, 1969) supplemented with 10 % foetal bovine serum (FBS). After cultivation for three and seven days respectively, 2×10^7 cells of each parasite were harvested by centrifugation (650 g × 8 minutes). The cells of each parasite were washed three times by centrifugation with 10 mM phosphate-buffered saline (PBS) (pH 7.4), and each pellet was suspended in approximately eight times its volume of 50 mM Tris-HCl (pH 7.4). *L. major* was axenically cultured in Schneider's medium (Gibco™) supplemented with 15 % FBS at 26° C for four days and harvested by centrifugation (650 g × 8 minutes). *A. castellanii* was axenically cultured in peptone-yeast glucose (PYG) medium (Rowbotham, 1983; ATCC media formulations No. 712) for four days and harvested by centrifugation (650 g × 4 minutes). The P388D1 cell line was cultured in RPMI 1640 medium (Nissui Pharmaceutical Co., Taito-ku, Tokyo, Japan) supplemented with 10 % FBS for four days and harvested by centrifugation (125 g × 4 minutes). *T. vaginalis* and *T. foetus* were axenically cultured for three days in BI-S-33 medium in which the peptone components of TYI-S-33 medium (Diamond *et al.*, 1978) are substituted by Biosate (BBL, Becton Dickinson Co., Cockeysville, Maryland, USA), and harvested by centrifugation (275 g × 4 minutes). The Cp-rich fraction from the wild spiderwort (*C. communis* L.) was isolated. The leaves of wild spiderwort were picked from the private field of Keio University (Tokyo) during the flower season from June to August (2000-2003). Fresh green spiderwort leaves were stripped from the stems, washed with tap water and then with distilled water. The leaves were ground with serum-free RPMI 1640 medium (RPMI) in an earthenware mortar by using a wooden pestle. The resulting leaf cell suspension was filtered through a double thickness gauze to remove the residue. The cell suspension was then washed three times with RPMI by centrifugation (440 g × 10 minutes). *P. aeruginosa* was cultured in Biosate-Iron broth (Diamond *et al.*, 1978) for three days and harvested by centrifugation (650 g × 4 minutes). *G. intestinalis* was axenically cultured in modified BI-S-33 medium (Keister, 1983) for three days and harvested by centrifugation (275 g × 4 minutes).

PREPARATION OF MT, HG AND CP FRACTIONS

Mt, Hg and Cp rich fractions were prepared as described by Hogeboom (1955), Opperdoes *et al.* (1984) and Gorham (1955), respectively. Since the methodology for mitosome isolation has not been established, intact cells of *G. intestinalis* were tested for their growth-promoting effect without preparing the mitosome rich fraction. After washing the fractions with RPMI once by centrifugation (440 g × 10 minutes), each fraction was suspended in 2 ml of RPMI. In order to test for their growth-promoting effect under axenic culture conditions, the fractions were sterilized by autoclaving (121° C, 15 minutes), and 0.2 ml of each suspension was added into the YIGADHA-S medium (5 ml). The

medium was then inoculated with a 0.8 ml suspension of *E. dispar* (AS16IR strain = AS 16 IR) (final density: 200-2,700 amoebae/ml).

NuPAGE® Novex 4-12 % Bis-Tris gradient peptide gel electrophoresis and preparative sodium dodecyl sulfate-polyacrylamide gel electrophoresis (SDS-PAGE)

The lyophilized cell fraction of spiderwort was extracted with 20 %, 40 %, 80 % and 100 % acetone solutions (20 mg/ml) for 10 minutes at 4° C. After centrifugation (17,800 g × 10 minutes, 4° C) of each acetone extract, the supernatant was collected. The supernatants that were extracted with 80 % and 100 % acetone solutions were diluted with distilled water to obtain an acetone concentration of 50 %. Each supernatant was then concentrated by evaporation by using a SpeedVac system (SVC 100; Savant Instruments, Inc., Farmingdale, New York, USA) until evaporated to dryness. The molecular weight of the proteins in each extract was determined by NuPAGE® Novex 4-12 % Bis-Tris gradient peptide (Invitrogen Corp., Carlsbad, California, USA) gel electrophoresis.

The bands of complexes of low molecular weight protein with chlorophyll that were detected in the supernatants of 80 % and 100 % acetone extracts were isolated by preparative SDS-PAGE on a 12 % gel in a Mini Prep Cell (Bio-Rad Laboratories, Inc., Hercules, California, USA) electrophoresis unit. SDS-PAGE was performed according to the procedure described by Laemmli (1970). For NuPAGE® (Novex 4-12 % gradient peptide gel = Novex 4-12 %) each dried and concentrated supernatant of the acetone extract was redissolved in the sample buffer with 50 mM dithiothreitol and heated at 70° C for 10 minutes to reduce the disulfide bonds. For SDS-PAGE (12 % gel) each supernatant was redissolved in the sample buffer with 1 % (v/v) 2-mercaptoethanol (2ME) and boiled for four minutes. Following NuPAGE®, the gel was stained with 2D-silverstain II (Daiichi Pure Chemicals Co. Ltd., Chuo-ku, Tokyo, Japan).

Assay of the acetone extracts of spiderwort leaf cells for a GPF

One millilitre supernatants (obtained after centrifugation; 17,800 g × 10 minutes, 4° C) of the 20 %, 40 %, 80 % and 100 % acetone extracts of the lyophilized cell fraction of spiderwort (20 mg/ml) was dialyzed three times against 200-250 volumes of distilled water for 18 hours by using a Spectra/Por® 3 (3500 MWCO) dialysis membrane for 18 h; the volume of each extract was adjusted to 2.4 ml. Each extract was sterilized by filtration (Sartorius membrane filter; 0.2-µm pore size), and 0.2 ml of each extract was added to the YIGADHA-S medium to test the growth-promoting effect of the extract on *E. dispar* (AS 16 IR).

Analysis using a scanning electron microscopy (SEM)/energy dispersive X-ray analyser (EDX)-integrated analysis system

Following the preparative SDS-PAGE, the complexes of chlorophyll with low molecular weight proteins in the 80 % and 100 % acetone-soluble fractions were dialyzed in the same manner as described above. After lyophilization, the dialyzed complexes were examined using an SEM and EDX-integrated analysis system SEM-EDX III Type N/H (Hitachi Science Systems, Ltd., Hitachinaka, Ibaragi, Japan) in the Nihonbashi laboratory, Hitachi High-Technologies Co., Tokyo, Japan.

Preparation of chlorophyll-a complexes with purified iron-sulphur proteins

Purified Fd from spinach (1 µg/µl; Sigma F-3013) and *C. pasteurianum* (1 µg/µl; Sigma F-7629) and purified rubredoxin (Rd) from *C. pasteurianum* (15.7 µg/µl; Sigma R-2512) were dissolved in 0.6 % 2ME/H_2O (20 µg of Fd or 31.4 µg of Rd/4 ml of 0.6 % 2ME), and the Fd and Rd solutions were dialyzed in the same manner as described above. Purified chlorophyll-a (Sigma C-5753) was dissolved in acetone (25 µg/25 µl acetone), and after adding 4 ml of distilled water, the solution was dialyzed in the same manner as described above. The Fd and Rd solutions were mixed with dialyzed chlorophyll-a and incubated for 10 minutes at 25° C. The solutions of chlorophyll-a complexes were then sterilized by filtration, and 0.2 ml of each solution was added to the YIGADHA-S medium to test their growth-promoting effect on *E. dispar* AS 16 IR.

Statistical analysis of growth-promoting effect on *E. dispar*

All experiments for testing growth-promoting effect were repeated at least twice. The data of each experiment were subjected to one-way analysis of variance (ANOVA) with Dunnett's multiple comparison post hoc test; the levels of statistical significance were taken as $p < 0.05$ and $p < 0.01$.

RESULTS

The Mt, Hg and Cp isolated from eight different types of cells were tested to determine whether they promoted the growth of axenically grown *E. dispar* AS 16 IR. The intact cells of *G. intestinalis* and *P. aeruginosa* were also tested for the same. A growth-promoting effect was apparently observed for every fraction except for the fraction of intact cells of *G. intestinalis*. Apparently, the intact cells of *E. histolytica* (HM-1: IMSS clone 6 strain) containing mitosomes (Leon-Avila & Tovar, 2004) also did not produce a

growth-promoting effect (data not shown). Although the growth-promoting effect of the two fractions of Mt from *T. cruzi* and the Hg fraction from *T. vaginalis* retained the statistically significant difference by Dunnett's test ($p < 0.05$), the growth-promoting effect of the other six fractions containing Mt, Hg and Cp was significantly different ($p < 0.01$ or $p < 0.05$). In particular, the effect of the Cp fraction from spiderwort exceeded that of the intact cells fraction of *P. aeruginosa* as shown in Figure 1. Thus, it was concluded that some of the Mt, Hg and Cp fractions, which were obtained under appropriate conditions as well as the intact bacterial cells contain a GPF.

Acetone extraction was used to obtain a water-soluble GPF from Cp-rich leaf cells of some plant species (e.g., spiderwort, cherry and morning glory), which have sufficiently strong leaf-cell membranes that can withstand the leaf crushing and cell isolation process. Figure 2 shows the results obtained on testing the 0 %, 20 %, 40 %, 80 % and 100 % acetone-soluble fractions from lyophilized Cp-rich leaf cells of spiderwort for a growth-promoting effect. The results showed that the 20 % and 80 % acetone-soluble fractions had a stronger growth-promoting effect than the other acetone-soluble fractions (0 %, 40 % and 100 %). The growth-promoting effects of the 20 % and 80 % acetone-soluble fractions were statistically significant at $p < 0.01$ (Dunnett's test); however, the effects of the 0 %, 40 % and 100 % acetone-soluble fractions were retained at $p < 0.05$. The silverstain NuPAGE® analysis of these acetone-soluble fractions yielded a distinct dense protein band (MW 4600) that was common to the 20 %, 40 %, 80 % and 100 % acetone-soluble fractions. The intensity of the bands of the 20 % and 80 % acetone-soluble fractions were stronger than the bands of the other acetone-soluble fractions (40 % and 100 %) (Fig. 3). These results indicated that the efficacy of the growth-promoting effect was correlated with the intensity of the low molecular weight protein band (Figs 2, 3). The band of the complex of the chlorophyll with low molecular weight proteins (green colour) present in both the 80 % and 100 % acetone-soluble fractions was obtained by SDS-preparative electrophoresis; both the fractions showed a growth-promoting effect on *E. dispar* AS 16 IR (data not shown). The result showed that the band of the complex of chlorophyll with low molecular weight proteins, which was present in the acetone-soluble fractions, contained a GPF. The reduction in the intensity of the low molecular weight protein bands obtained by using the 40 % acetone-soluble fraction was considered to be caused by the incomplete solubility of chlorophyll. Some protein parts are believed to be precipitated together with the insoluble chlorophyll when extraction is performed with an intermediate concen-

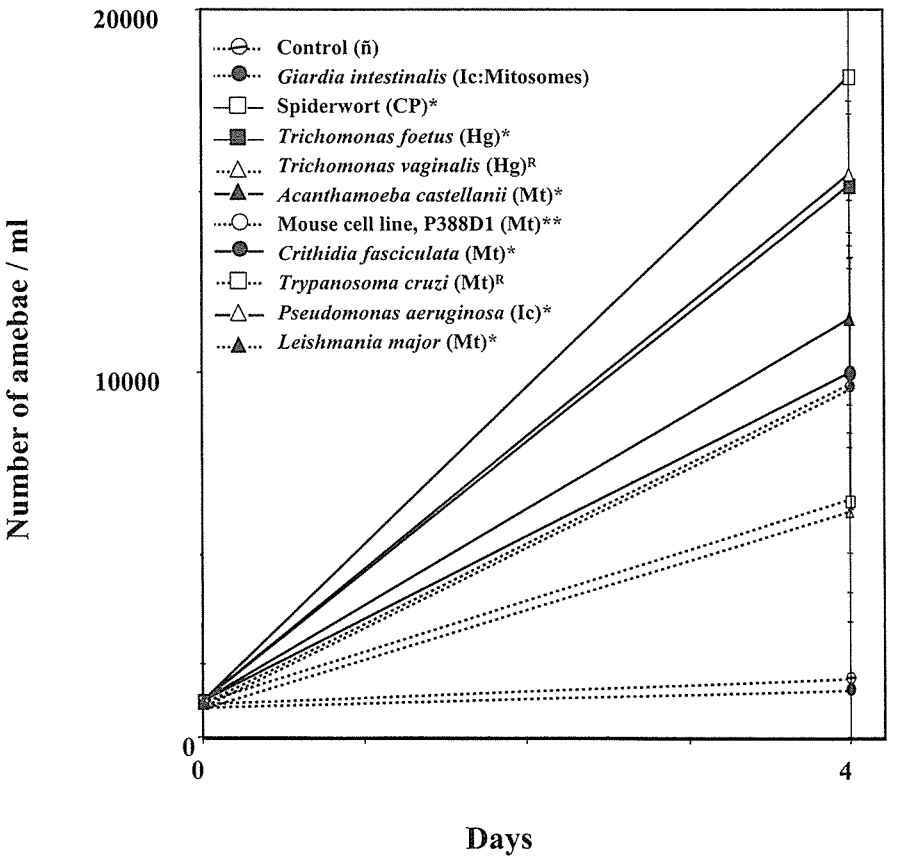

Fig. 1. – The effect of intact cells (Ic) and the fractions of mitochondria (Mt), chloroplasts (Cp) and hydrogenosomes (Hg) from ten types of cells, including bacterial, mammalian, plant and protozoan cells, on the growth of *Entamoeba dispar*.
The cellular components were sterilized by autoclaving at 121° C for 15 minutes. The growth kinetics of the *E. dispar* AS 16 IR strain in the YIGADHA-S medium are shown (mean numbers of amoebae in duplicate cultures are plotted). *, **: the mean of the growth-kinetic level was significantly higher than that of the control (*$p < 0.01$ and **$p < 0.05$ by Dunnett's test). R: the significant difference was retained by Dunnett's test ($p < 0.05$).

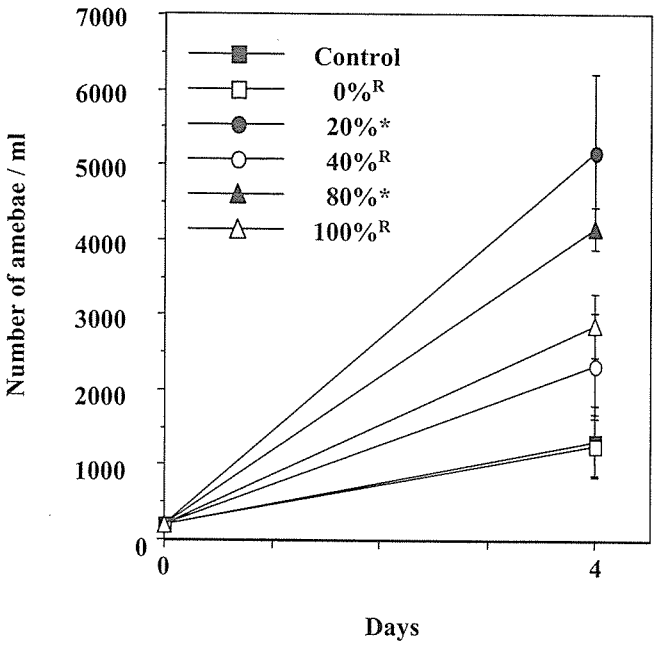

Fig. 2. – Effect of soluble fractions of spiderwort Cp-rich leaf cells extracted with five different concentrations of acetone (0 %, 20 %, 40 %, 80 % and 100 %) on the growth of *E. dispar*.
The growth kinetics of the *E. dispar* AS 16 IR strain in the YIGADHA-S medium are shown (mean numbers of amoebae in duplicate cultures are plotted). *: the mean of the growth-kinetic level was significantly higher than that of the control (*$p < 0.01$ by Dunnett's test). R: the significant difference was retained by Dunnett's test ($p < 0.05$).

tration of acetone such as 40 %. As compared to an 80 % acetone concentration, the 100 % concentration of acetone was considered to be slightly severe for the extraction of the low molecular weight proteins without decreasing the activity of a GPF. As a result, the intensity of the low molecular weight protein bands obtained by using the 40 % and 100 % acetone-soluble fraction was believed to be reduced.

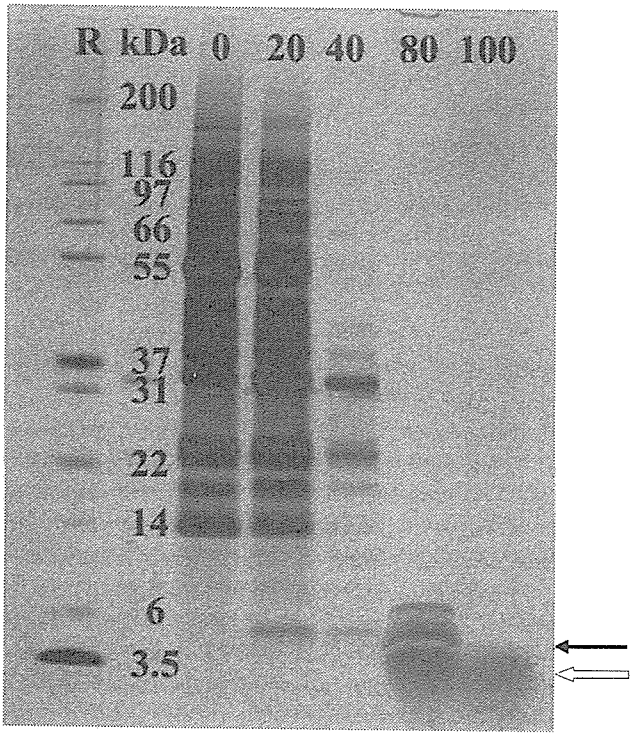

Fig. 3. – NuPAGE® (Novex 4-12 %) of five acetone-soluble fractions of spiderwort Cp-rich leaf cells extracted with different concentrations of acetone (0 %, 20 %, 40 %, 80 % and 100 %).
Molecular mass markers (M) are shown on the left. ⟵ : acetone-soluble low molecular weight protein bands were isolated from the 20 %, 40 %, 80 % and 100 % acetone-soluble fractions. ⟸ : broad green band of chlorophyll.

The SEM/EDX-integrated analysis system revealed that the low molecular weight protein band contained Fe, S and Mo atoms along with the Mg atom of chlorophyll (Figs 4, 5). We believed that Fd present in Cp is a type of Fe-S protein containing Fe and S atoms. In order to confirm the growth-promoting effect of Fd, we examined the effects of purified spinach Fd (MW 12,000), *C. pasteurianum* Fd (MW 6,000) and purified *C. pasteurianum* Rd (MW 19,000) on the growth of *E. dispar* AS 16 IR. The analysis revealed that 0.6 % 2ME-treated *C. pasteurianum* Rd and each of the water-soluble chlorophyll-a complexes with 0.6 % 2ME-treated spinach Fd and *C. pasteurianum* Fd have a growth-promoting effect on *E. dispar* AS 16 IR with a statistically significant difference ($p < 0.01$) (Fig. 6). The non-complexed Fd from spinach and from *C. pasteurianum* treated with 0.6 % 2ME also had a slight growth-promoting effect when compared with the growth kinetics of the control with or without chlorophyll-a; however, these growth-promoting effects were retained ($p < 0.05$).

These results suggest that the GPF in the acetone-soluble fraction of spiderwort Cp-rich leaf cells is the complex of the chlorophyll-a with a component of an Fe-S protein, such as an inorganic Fe-S centre, released by the breakage of disulfide bonds due to treatment with 2ME. The Fe-S redox proteins are commonly found in enteric bacteria (e.g., Fd), mitochondria (e.g., Fe-S proteins in complex I and II), chloroplasts (e.g., Fd) and hydrogenosomes (e.g., Fd); however, there are diffe-

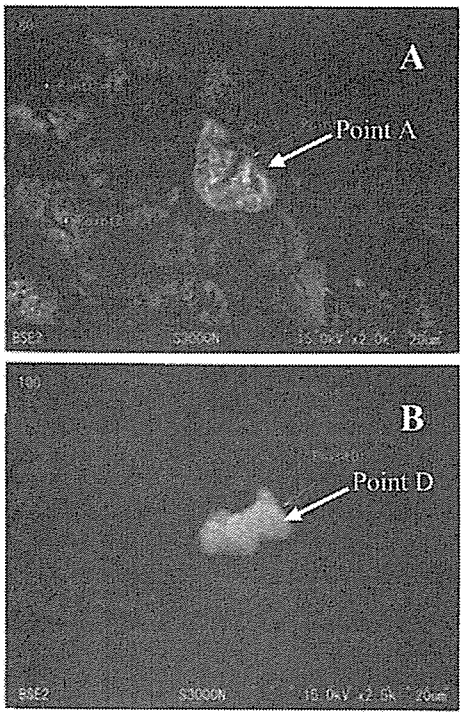

Fig. 4. – Scanning electron microscope (SEM) images of crystals observed in complexes of chlorophyll with low molecular weight proteins present in the 80 % (A) and 100 % (B) acetone-soluble fractions.
By using an SEM/energy dispersive X-ray (EDX) analyzer, Fe atoms were detected at point A (A) and S and Mo atoms were detected at point D (B).

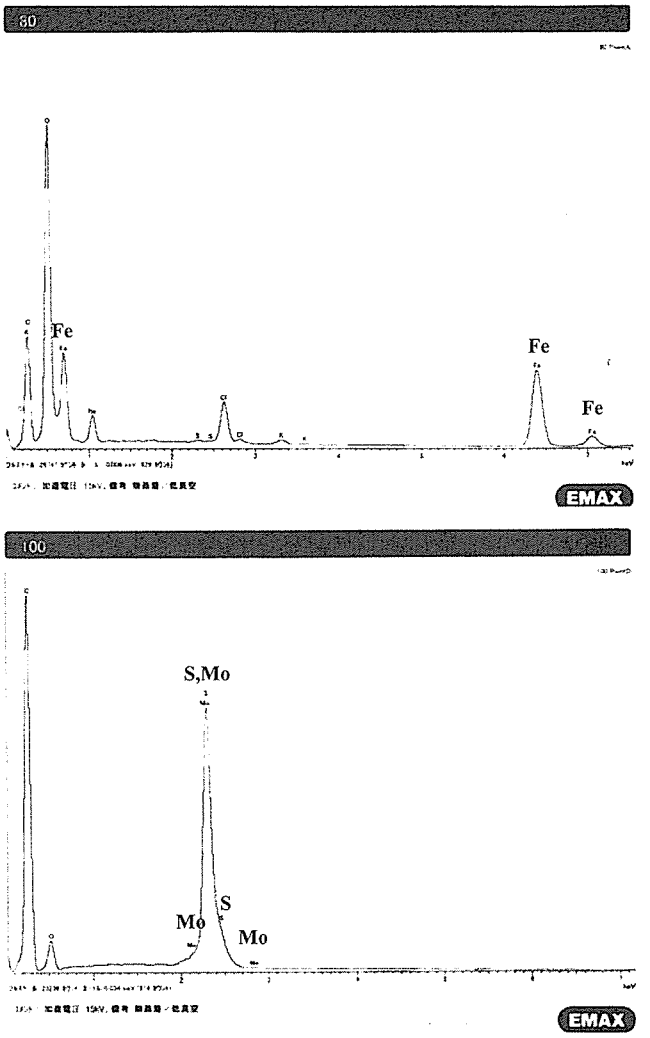

Fig. 5. – Specific peaks of the Fe atom at point A (Fig. 3) and S and Mo atoms at point D (Fig. 3) detected in the complexes of chlorophyll with low molecular weight proteins in the 80 % (A) and 100 % (B) acetone-soluble fractions by using an SEM/EDX analyzer.

rences in the chemical structure of their Fe-S centers. In *E. dispar*, Fd is considered as an essential redox protein involved in energy metabolism, similar to that in *E. histolytica*, although neither species contains Mt. These findings suggest that *E. dispar* grown under axenic culture conditions may lack a sufficient quantity of some essential component of the Fe-S proteins (e.g., Fe-S centre).
The growth-promoting effect of the GPF was tested on three other strains of *E. dispar* (SAW 1734R clone AR, AS 2 IR and CYNO 16:TPC), (Koyabashi *et al.*, 2005); it was confirmed that the GPF produced the same effect on their growth (data not shown).

DISCUSSION

Previously, we designed the YIGADHA-S medium (Kobayashi *et al.*, 2005) for axenic cultivation of *E. dispar*. It contains dihydroxyacetone (DHA) that has a significant growth-promoting effect on *E. dispar*. DHA is a ketotriose and functions as a sugar source for *E. dispar*; therefore, it is considered to be directly metabolized to DHA phosphate, which is an intermediary metabolite in the Embden-Meyerhof-Parnas glycolytic pathway. However, the growth of *E. dispar* was poor despite the presence of DHA.
In the present study, a GPF was detected in the autoclaved Mt, Hg and Cp fractions and in intact bacteria and was demonstrated to show a growth-promoting effect on *E. dispar*. However, the efficacy of each GPF from these organelles varied under different conditions. Prior to the present study, detection of a GPF from trophozoites of *E. histolytica* (HM-1:IMSS clone 6 strain) was attempted. Since *E. histolytica* is genetically closely related to *E. dispar*, it contains an abundance of Fe-S proteins, such as Fd, which are only stable under anaerobic conditions, and it contains mitochondrial remnant mitosomes (Leon-Avila & Tovar, 2004). However, neither the intact cells nor any extract from the cells could promote the growth of *E. dispar* AS 16 IR (data not shown). One reason for the failure to extract a GPF from *E. histolytica* trophozoites may be the fragility of

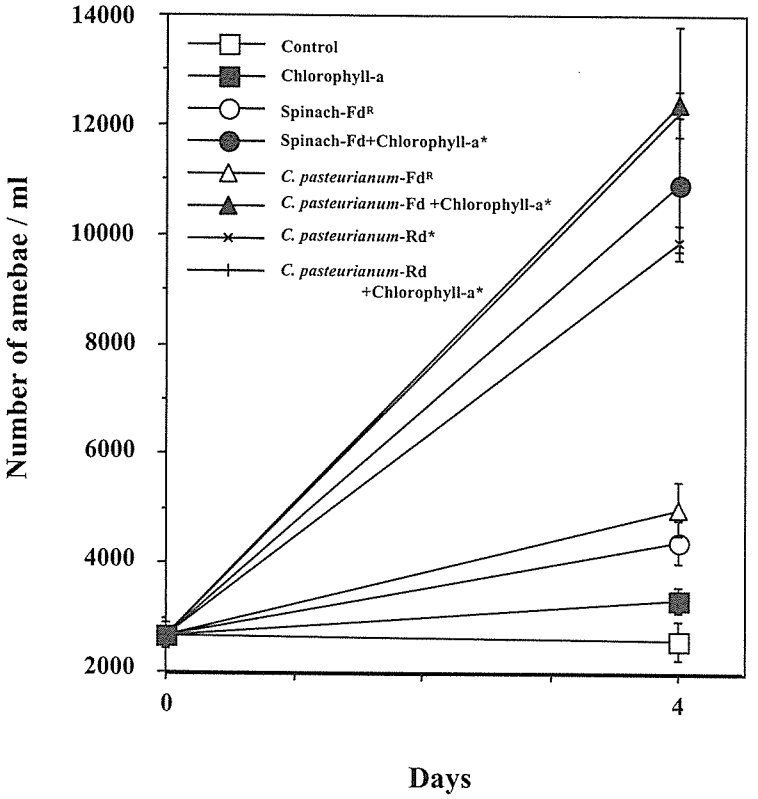

Fig. 6. - Effect of chlorophyll-a (—■—), 0.6 % 2ME-treated spinach ferredoxin (Fd) (—○—), *Clostridium pasteurianum* Fd (—△—) and *C. pasteurianum* rubredoxin (Rd) (—×—), and complexes of chlorophyll a with spinach Fd (—●—), *C. pasteurianum* Fd (—▲—) and *C. pasteurianum* Rd (—+—) on the growth of *E. dispar*, and control (—□—).
The growth kinetics of the *E. dispar* AS 16 IR strain in the YIGADHA-S medium are shown (mean numbers of amoebae in duplicate cultures are plotted). *: the mean of the growth-kinetic level was significantly higher than that of the control (*$p < 0.01$ by Dunnett's test). R: the significant difference was retained by Dunnett's test ($p < 0.05$).

the cell membrane and organelles (e.g.,mitosomes) similar to that of the spinach leaf cells. The GPF was assumed to be composed of a heat-stable substance and some other common simple inorganic substances. It was feasible to isolate the GPF from acetone-soluble fractions of Cp-rich leaf cells as bands of low molecular weight proteins complexed with chlorophyll containing Fe, S and Mo atoms.

The results of this study indicate that the protein bands may be derived from Fe-S (e.g., Fd) or Mo-Fe-S proteins [e.g., molybdoferredoxin, which is a common component of nitrogenase (present in rhizobium species)]. It appears that the GPF requires to form a complex with chlorophyll because the growth-promoting effects of purified Fd from spinach, *C. pasteurianum* and *E. histolytica* strain HM-1: IMSS clone 6 (the Fd consists of 4Fe-4S centre) on *E. dispar* AS 16 IR were not remarkable (data not shown). We found that the complex of chlorophyll-a with 0.6 % 2ME-treated Fd containing a 2Fe-2S centre from spinach and that containing 4Fe-4S centre from *C. pasteurianum* have a growth-promoting effect on *E. dispar* AS 16 IR. This effect was also observed with 0.6 % 2ME-treated Rd, which has the most simple Fe-S centre (1 Fe and 4 cysteine-residues without inorganic S), without chlorophyll-a. It is not clearly understood why complex formation must occur between chlorophyll-a and the components (Fe-S centres and cysteine residues) of bacterial and plant Fd to produce a growth-promoting effect is not clearly understood. However, it is considered that the complex of chlorophyll-a with the Fd component (MW greater than 100,000 by gel permeation chromatography) may be efficiently taken up by amoeba cells as a compact mass by a process, such as pinocytosis, and the complex may be degraded until an appropriate size of the Fe-S compound is obtained. We speculate that the Fe-S compounds are utilized as components of some essential Fe-S proteins such as amoebic Fd, which is an essential redox protein involved in oxidative decarboxylation of pyruvate to acetyl CoA in *E. dispar*; this is similar to that reported in *E. histolytica* (McLaughlin & Aley, 1985). It is reported that the amitochondrial protozoan parasite *E. histolytica*, which is closely related to *E. dispar*, contains numerous fermentation enzymes that are similar to bacterial enzymes, including the pyruvate Fd oxidoreductase, Fd and alcohol dehydrogenase E, derived from concomitant enteric bacterial DNA by horizontal transfer (Rosenthal *et al.*, 1997).

We succeeded in developing a more stable axenic cultivation system by adding the complex of chlorophyll with a component of Fe-S protein (e.g., Fd from spiderwort) treated with 2ME to the YIGADHA-S medium. We achieved an improved axenic cultivation system *for E. dispar* by using cellular components of protozoan, mammalian and plant cells as well as intact bacteria. However, we recognize that it is difficult to develop an axenic cultivation system for *E. dispar* that is at par

with the well-established cultivation system of *E. histolytica* for use in biological studies such as biochemical and immunological studies, etc.

ACKNOWLEDGEMENTS

The authors thank the staff of Nihonbashi Laboratory, Hitachi High-Technologies Co., Tokyo, Japan for their cooperation in the analysis using the SEM-EDX III Type N/H. This work was supported by a Keio Gijuku Fukuzawa Memorial Fund for the Advancement of Education and Research and a Health Sciences Research Grant-in-Aid for Emerging and Reemerging Infectious Diseases.

REFERENCES

CLARK C.G. Axenic cultivation of *Entamoeba dispar* Brumpt 1925, *Entamoeba insolita* Geiman and Wichterman 1937 and *Entamoeba ranarum* Grassi 1879. *Journal of Eukaryotic Microbiology*, 1995, *42*, 590-593.

DIAMOND L.S., HARLOW D.F. & CUNNICK C.C. A new medium for the axenic cultivation of *Entamoeba histolytica* and other *Entamoeba*. *Transactions of the Royal Society of Tropical Medicine and Hygiene*, 1978, *72*, 431-432.

DIAMOND L.S. A new liquid medium for xenic cultivation of *Entamoeba histolytica* and other lumen-dwelling protozoa. *Journal of Parasitology*, 1982, *68*, 958-959.

DIAMOND L.S., CLARK C.G. & CUNNICK C.C. YI-S, a casein-free medium for axenic cultivation of *Entamoeba histolytica*, related *Entamoeba*, *Giardia intestinalis* and *Trichomonas vaginalis*. *Journal of Eukaryotic Microbiology*, 1995, *42*, 277-278.

GORHAM P.R. Preparation of chloroplasts and disintegrated chloroplasts, *in*: Methods in Enzymology vol. I. Colowick S.P. & Kaplan N.O. (eds), Academic Press, New York, 1955, 22-25.

GUTTERIDGE W.E., KNOWLER J. & COOMBES J.D. Growth of *Trypanosoma cruzi* in human heart tissue cells and effects of aminonucleoside of puromycin, trypacidin and aminopterin. *Journal of Protozoology*, 1969, *16*, 521-525.

HOGEBOOM G.H. Fractionation of cell components of animal tissues, *in*: Methods in Enzymology vol. I. Colowick S.P. & Kaplan N.O. (eds), Academic Press, New York, 1955, 16-19.

KEISTER D.B. Axenic culture of *Giardia lamblia* in TYI-S-33 medium supplemented with bile. *Transactions of the Royal Society of Tropical Medicine and Hygiene*, 1983, *77*, 487-488.

KOBAYASHI S., IMAI E., HAGHIGHI A., KHALIFA S.A., TACHIBANA H. & TAKEUCHI T. Axenic cultivation of *Entamoeba dispar* in newly designed yeast extract-iron-gluconic acid-dihydroxyacetone-serum medium. *Journal of Parasitology*, 2005, *91*, 1-4.

KOBAYASHI S., IMAI E., TACHIBANA H., FUJIWARA T. & TAKEUCHI T. *Entamoeba dispar*: cultivation with sterilized *Crithidia fasciculata*. *Journal of Eukaryotic Microbiology*, 1998, *45*, 3S-8S.

KOBAYASHI S., IMAI E., HAGHIGHI A., TACHIBANA H. & TAKEUCHI T. Cultivation of *Entamoeba dispar*: growth-promoting effect of ferredoxin. *Archives of Medical Research*, 2000, *31* (Suppl.), S210-S211.

LAEMMLI U.K. Cleavage of structural proteins during the assembly of the head of bacteriophage T4. *Nature*, 1970, *227*, 680-685.

LEON-AVILA G. & TOVAR J. Mitosomes of *Entamoeba histolytica* are abundant mitochondrion-related remnant organelles that lack a detectable organellar genome. *Microbiology*, 2004, *150*, 1245-1250.

MCLAUGHLIN J. & ALEY S. The biochemistry and functional morphology of the *Entamoeba*. *Journal of Protozoology*, 1985, *32*, 221-240.

OKAMOTO S., WAKUI M., KOBAYASHI H., SATO N., ISHIDA A., TANABE M., TAKEUCHI T., FUKUSHIMA S., YAMADA T. & IKEDA Y. *Trichomonas foetus* meningoencephalitis after allogeneic peripheral blood stem cell transplantation. Bone Marrow *Transplantation*, 1998, *21*, 89-91.

OPPERDOES F.R., BAUDHUIN P., COPPENS I, DE ROE C., EDWARDS S.W., WEIERS P.J. & MISSET O. Purification, morphometric analysis, and characterization of glycosomes (microbodies) of the protozoan hemoflagellate *Trypanosoma brucei*. *Journal of Cell Biology*, 1984, *98*, 1178-1184.

QI H.Y., KOBAYASHI S., FUJIWARA T., NOZAWA S., OHTA H., KIGUCHI K., TOJO R., KOBAYASHI J., SUMI K., YANO A. & TAKEUCHI T. Occurrence of metronidazole-resistant *Trichomonas vaginalis* in Japan. *Japanese Journal of Parasitology*, 1995, *44*, 473-480.

ROBINSON G.L. The laboratory diagnosis of human parasitic amoebae. *Transactions of the Royal Society of Tropical Medicine and Hygiene*, 1968, *62*, 285-294.

ROSENTHAL B., MAI Z., CAPLIVSKI D., GHOSH S., DE LA VEGA H., GRAF T. & SAMUELSON J. Evidence for the bacterial origin of genes encoding fermentation enzymes of the amitochondriate protozoan parasite *Entamoeba histolytica*. *Journal of Bacteriology*, 1997, *179*, 3736-3745.

ROWBOTHAM T.J. Isolation of *Legionella pneumophila* from clinical specimens via amoebae, and the interaction of those and other isolates with amoebae. *Journal of Clinical Pathology*, 1983, *36*, 978-986.

TOVAR J., LEON-AVILA G., SANCHEZ L.B., SUTAK R., TACHEZY J., VAN DER GIEZEN M., HERNANDEZ M., MULLER M. & LUCOCQ J.M. Mitochondrial remnant organelles of *Giardia* function in iron-sulphur protein maturation. *Nature*, 2003, *426*,172-176.

VARGAS M.A., ISIBASI A., KUMATE J. & OROZCO E. Non-pathogenic *Entamoeba histolytica*: functional and biochemical characterization of a monoxenic strain. *Molecular and Biochemical Parasitology*, 1990, *40*, 193-201.

Reçu le 14 juin 2005
Accepté le 4 novembre 2005

CLINICAL MICROBIOLOGY REVIEWS, Jan. 2007, p. 164–187 Vol. 20, No. 1
0893-8512/07/$08.00+0 doi:10.1128/CMR.00019-06

Current Therapeutics, Their Problems, and Sulfur-Containing-Amino-Acid Metabolism as a Novel Target against Infections by "Amitochondriate" Protozoan Parasites

Vahab Ali and Tomoyoshi Nozaki*

Department of Parasitology, Gunma University Graduate School of Medicine, 3-39-22 Showa-machi, Maebashi, Gunma 371-8511, Japan

INTRODUCTION

Three protozoan parasites of humans, *Entamoeba histolytica*, *Giardia intestinalis*, and *Trichomonas vaginalis*, share various biological and biochemical characteristics, including anaerobic carbohydrate metabolism and the lack of typical mitochondria ("amitochondriate"). The ATP generation in these parasites occurs exclusively through substrate-level phosphorylation, despite differences in their life cycles and pathogenic properties (216, 217). As obligatory parasites, these organisms have a reduced ability for the de novo synthesis of essential building blocks of DNA and proteins, including nucleic acid precursors (7, 10, 322) and amino acids (7, 233, 247). As a consequence, certain metabolic pathways either are missing in these organisms or are divergent from those of mitochondriate organisms. Sulfur-containing-amino-acid metabolism represents one such divergent metabolic pathway in these three "amitochondriate" protists. Sulfur-containing amino acids are essential for a variety of biological activities, including protein synthesis, methylation, polyamine synthesis, coenzyme A production, cysteamine production, taurine production, iron-sulfur cluster (ISC) biosynthesis, and antioxidative stress defense (233). Besides the general importance of sulfur-containing amino acids, it was previously shown that a high concentration of extracel-

* Corresponding author. Mailing address: Department of Parasitology, Gunma University Graduate School of Medicine, 3-39-22 Showa-machi, Maebashi, Gunma 371-8511, Japan. Phone: 81-27-220-8020. Fax: 81-27-220-8025. E-mail: nozaki@med.gunma-u.ac.jp.

lular cysteine is required for the growth, attachment, and survival of *E. histolytica*, *T. vaginalis*, and *G. intestinalis* under oxidative stress (2, 36, 106–110, 298).

Recent molecular and biochemical characterization of the sulfur-containing-amino-acid metabolism in these organisms revealed that metabolic pathways for sulfur-containing amino acids in *E. histolytica*, *G. intestinalis*, and *T. vaginalis* are distinct from those of their mammalian hosts in several ways. First, they lack part of both the forward and reverse transsulfuration pathways and thus are unable to complete transsulfuration sequences in either direction between methionine and cysteine. Second, they lack the enzymes responsible for cysteine and homocysteine degradation in mammals. Instead, *E. histolytica* and *T. vaginalis* possess a unique enzyme for the degradation of methionine, homocysteine, and cysteine called methionine γ-lyase. Third, *E. histolytica* and *T. vaginalis* are capable of sulfur-assimilatory de novo cysteine biosynthesis. Since aspects of sulfur-containing-amino-acid metabolism differ significantly between parasites and their mammalian hosts, molecular dissection and characterization of the unique properties of the sulfur-containing-amino-acid metabolism of these "amitochondriate" parasites should lead to the exploitation of new chemotherapeutic agents against infections caused by these pathogens. This review discusses the current therapeutic agents against infections by these "amitochondriate" protozoan parasites, their targets and mode of action, and the molecular mechanism of drug resistance. We also summarize various aspects of the unique sulfur-containing-amino-acid metabolism in these protozoa and discuss how these metabolic pathways could be exploited as novel targets for development of drugs against these infections.

EPIDEMIOLOGY, BIOLOGY, AND DISEASE

Entamoeba histolytica

The World Health Organization (WHO) estimated that 280 million people are infected each year and 2.5 million deaths occur annually from diarrheal diseases (314, 333). *Entamoeba histolytica* is an enteric unicellular protozoan parasite belonging to the Entamoebidae family. It causes amoebic colitis and extraintestinal abscesses in approximately 50 million inhabitants of areas of endemicity, resulting in an estimated 40,000 to 110,000 deaths annually and making this disease the second leading cause of death from parasitic diseases (321; WHO/PAHO/UNESCO report, presented at the WHO/PAHO/UNESCO meeting, Mexico City, Mexico, 28 to 29 January 1997). Other than imported cases, *E. histolytica* infection is rarely found in most industrialized countries, although infection with the closely related but commensal (noninvasive) species *Entamoeba dispar* is frequently found in these countries. *E. dispar* does not usually invade tissues and at most produces only superficial erosion of the colonic mucosa. In developed countries, travelers and immigrants are at risk of amoebiasis infections (293). In some developed countries, amoebiasis is domestically transmitted only in the restricted populations of the mentally handicapped and male homosexuals (232, 236).

E. histolytica has a simple life cycle consisting of two stages, an infective cyst stage and a proliferating trophozoite form. Human and certain nonhuman primates are its only natural hosts. Infection of the host occurs upon ingestion of water or food contaminated with cysts. *E. histolytica* cysts are round, usually 10 to 15 μm in diameter, and surrounded by a refractive wall containing chitin. After ingestion, the cyst excysts in the small intestine and forms the amoeboid trophozoite, which then colonizes the large intestine of the host. Colonization by *E. histolytica* trophozoites often results in an asymptomatic intestinal infection similar to that resulting from *E. dispar* (67). Unlike the inert cysts, *E. histolytica* trophozoites are highly motile, with polymorphic shapes and sizes varying from 10 to 50 μm in diameter. Trophozoites reproduce by binary fission, ingest bacteria and food particles, and adhere to and destroy epithelial cells in the bowel. The destruction of the epithelial tissue causes disease and symptoms. After penetration into the blood vessels, trophozoites are occasionally transported to extraintestinal organs, including the liver, lung, brain, and skin, and produce abscesses, often with lethal outcomes. Trophozoites transform into dormant and infectious cysts which are excreted into the environment. Although signals leading to encystation and excystation of *E. histolytica* are still poorly understood, osmolality changes, nutrient depletion (278), and adherence via galactose-binding lectin (79) are likely involved in encystation. In vitro encystation of the related reptilian species *Entamoeba invadens* was established by manipulating osmotic and nutrient conditions of axenic cultures (20, 278, 317). However, encystation has not been achieved with an axenic *E. histolytica* line.

Many individuals infected with *E. histolytica* have no symptoms and clear their infection without disease. However, up to 10% of asymptomatic infected individuals develop disease within a year of being infected (293). Clinical symptoms of amoebic colitis include bloody diarrhea and abdominal pain and tenderness. Multiple mucoid stools are common and are almost invariably heme positive. Fever is unusual except in cases with concurrent amoebic liver abscess. Fulminant amoebic colitis characterized by profuse bloody diarrhea, fever, pronounced leucocytosis, and severe abdominal pain is occasionally seen in individuals at risk, including pregnant women, immunocompromised individuals, patients receiving corticosteroids, and individuals with diabetes and alcoholism. Liver abscess is the most common extraintestinal manifestation of amoebic infection, most likely caused by hematogenous spread of amoebic trophozoites from the colon. Symptoms associated with amoebic liver abscess are fever, right upper quadrant pain, and hepatic tenderness and sometimes include cough, anorexia, and weight loss. Pleuropulmonary amoebiasis may also develop when an amoebic liver abscess is ruptured through the diaphragm. Patients with pleuropulmonary amoebiasis have chest pain, pleural effusions, atelectasis, and respiratory distress. Rupture into the peritoneum occurs occasionally, leading to peritonitis and shock in some individuals with amoebic liver abscess. Patients with amoebic liver abscess infrequently develop rupture into the pericardium, leading to pericarditis, dyspnoea, tachycardia, and cardiac tamponade. Amoebic brain abscess, although very rare, may also occur with concomitant amoebic liver abscess. Clinical symptoms include headache, vomiting, and seizures. The onset and progression of amoebic brain abscess is very rapid, and outcomes are often lethal. Comprehensive reviews of the pathophysiology and clinical signs and symptoms are found elsewhere (122, 293).

E. histolytica is considered to be anaerobic or microaerophilic because it is sensitive to oxygen yet is able to reduce it to water (296). *E. histolytica* can grow only under reduced oxygen tension in vitro (325). Toxic reactive oxygen derivatives, including superoxide, are produced by the electron transfer that occurs during energy metabolism. *E. histolytica* possesses iron-containing superoxide dismutase (SOD) (39) for the detoxification of reactive oxygen intermediates, but it lacks catalase, peroxidase, and enzymes for glutathione synthesis and metabolism (92, 205, 325), which are almost ubiquitously present in aerobes and are responsible for the removal of hydrogen peroxide. However, *E. histolytica* possesses alternative mechanisms for detoxification of the reactive oxygen species. The alternative mechanism depends on reducing agents (thiols), especially cysteine. In glutathione-depleted medium, cysteine was the main thiol compound in *E. histolytica* and was present largely in the thiol rather than the disulfide form (92). As mentioned above, extracellular cysteine is required to maintain a reducing environment and is essential for growth, attachment, and survival of *E. histolytica* trophozoites. It is conceivable that cysteine and other, as-yet-uncharacterized thiols are involved in the regulation of antioxidative defense mechanisms that likely consist of SOD (39, 297), peroxiredoxin (a thiol-specific antioxidant) (323), p34 NADPH oxidoreductase (38), and rubrerythrin (185, 205). However, several key components of the pathway have not been identified, e.g., a reducing system for peroxiredoxin and rubrerythrin.

Giardia intestinalis

G. intestinalis, also known as *Giardia lamblia* or *Giardia duodenalis*, is a flagellated protist that belongs to the order Diplomonadida and is the most commonly detected protozoan parasite in the intestinal tract (199). *G. intestinalis* infects >40 animal species, and the disease is considered zoonotic (199). WHO estimates that 280 million people are infected each year with *G. intestinalis* (314, 333). The prevalence is very high in children in developing countries but decreases to 2 to 7% in developed nations (95, 199). Water- and food-borne transmission is the main route of transmission of giardiasis in developing countries (241). While food-borne outbreaks of *Giardia* infections are common in developing countries, waterborne outbreaks have occurred and could reoccur in developed countries (25, 212). Waterborne infections can be prevented by proper filtration of surface water supplies. It has also been reported that in certain areas of world, water contaminated with *G. lamblia* cysts commonly causes travel-related giardiasis in tourists (33). In addition, direct person-to-person transmission via a fecal-oral route during sexual intercourse, in the mentally handicapped population, and in day care settings has been demonstrated (7, 246).

The life cycle of *G. intestinalis* consists of two stages, an infective cyst and a proliferating trophozoite form. The cyst is the infective form of the parasite and can survive in water for several months (320). The ingested cyst excysts in the duodenum and then becomes a motile trophozoite after passing through the acidic environment of the stomach. The trophozoite reproduces by binary fission and attaches to the duodenal or jejunal mucosa (7, 8, 88), where it causes symptoms. Environmental stimuli, including cholic acid and low cholesterol, induce trophozoites to encyst (111, 189). However, the biochemical and physiological significance of cholesterol deprivation and the role of bile salts and fatty acids in the encystation process remain controversial. For the related issues of encystation and excystation of *G. intestinalis* and *E. histolytica*, recent reviews should be consulted (7, 78).

A range of symptoms, including nausea, vomiting, stomach cramps, and diarrhea, occur after an incubation period of 1 to 2 weeks. The acute phase of infection usually lasts 3 to 4 days, but symptoms sometimes persist for a longer period (8). In children, a failure-to-thrive syndrome caused by infection with high parasite burdens and malnutrition occasionally results in severe loss of body weight (up to 20%) (95). Thus, in the developing world, giardiasis is considered to be an important cause of morbidity (43). In the small intestine, infestation with the organism reduces the number of microvilli and the surface area at the brush border, causing atrophy of the villi and enterocyte immaturity. It also decreases disaccharidase and other luminal enzymes and causes malabsorption of electrolytes (43). A number of other symptoms are associated with giardiasis (43), but it is unlikely that these symptoms are causally connected to the infection. Consult recent reviews for updates on the pathogenesis, pathology, and cell biology of giardiasis (280).

The pathogenesis of giardiasis is partially attributable to the enzymes produced by the parasite, including serine and cysteine proteases which disrupt the epithelial barrier in the intestine, causing inflammation and an immune response in the host. *Giardia* trophozoites induce apoptosis of enterocytes, which is associated with disruption of the cytoskeleton and tight junctions. It has also been reported that disruption of cellular F-actin and ZO-1 in tight junctions and the concurrent increase in enterocyte permeability are modulated by caspase-3 and myosin light chain kinase. *Giardia* proteases are proposed to activate protease-activated receptor 1, a unique class of G protein-coupled signaling receptors which modulate apoptosis and increase enterocyte permeability (280).

Trichomonas vaginalis

T. vaginalis is a flagellated protozoan parasite belonging to the Trichomonadidae family. Worldwide, it is responsible for 180 million trichomoniasis infections annually (261). Trichomoniasis is a sexually transmitted disease (STD) of the genital tract, and the reported prevalence is extremely high in some developing countries. During an antenatal class in a rural region of South Africa, 65% of pregnant women were reportedly severely infected with *T. vaginalis* (135, 279). It was also reported that 67% of women who visited an STD clinic in Ulaanbaatar, Mongolia, were infected with *T. vaginalis* (281, 282). *T. vaginalis* was isolated from 14% to 60% of the male partners of infected women and from 67% to 100% of the female partners of infected men. Trichomoniasis is often associated with human immunodeficiency virus (HIV)/AIDS transmission and is known to be worsened by HIV infection (91, 211, 282, 292). In addition to venereal infection, rare cases of perinatal transmission have also been reported (121, 198).

The *T. vaginalis* life cycle consists of a single dividing trophozoite stage; no dormant (e.g., cyst) stage has been identified in this parasite. The trophozoite varies in size and shape, with an average length and width of 10 μm and 7 μm, respec-

tively (134). In axenic culture, the shape of the trophozoite tends to be more uniform, e.g., pear or oval shaped, but the parasite takes on a more amoeboid appearance when attached to vaginal epithelial cells (19, 124). The trophozoite has four free anterior flagella [9(2) + 2 arrangement] and a single recurrent flagellum incorporated into an undulating membrane which is supported by a noncontractile costa (282). The trophozoite divides by binary fission (247).

T. vaginalis infection in women ranges from an asymptomatic carrier state to profound acute inflammatory disease (261). The parasite generally infects the squamous epithelium of the genital tract, but it is occasionally recovered from the urethra, fallopian tubes, and pelvis (117, 247). The incubation period is 4 to 28 days in about 50% of infected individuals (247). The clinical picture in acute infection includes vaginal discharge, odor, and edema or erythema. The discharge is classically described as frothy, but actually it is frothy in only 10% of patients (282). Small punctuate hemorrhagic spots may be found on the vaginal and cervical mucosae in 2 to 3% of patients. These signs and symptoms are cyclic and worsen around the time of menses. Other complications associated with trichomoniasis include adnexitis, pyosalpinx, and endometritis (260); infertility and low birth weight (123); and cervical erosion (204). In males, *T. vaginalis* infection is often asymptomatic but occasionally causes urethritis and prostatitis (166). Urogenital trichomoniasis in men is categorized into three groups: an asymptomatic carrier state identified through an investigation of the sexual contacts of infected women, acute trichomoniasis characterized by profuse purulent urethritis, and mild symptomatic disease which is clinically indistinguishable from other causes of nongonococcal urethritis. The duration of infection is 10 days or less in most male patients. In symptomatic men, common complaints include scanty clear to mucopurulent discharge, dysuria, and mild pruritus or a burning sensation immediately after sexual intercourse (166). Complications associated with trichomoniasis include nongonococcal urethritis, prostatitis, balanoposthitis, urethral disease, and infertility (131, 167, 197). Pneumonia, bronchitis, and oral infection caused by *T. vaginalis* have also been documented (132). In rare cases, respiratory infections are acquired perinatally from infected mothers (132, 158). In children, *T. vaginalis* can infect the urinary tract as well as the vagina. It has been suggested that *T. vaginalis* infection is associated with sterility, but there is no unequivocal report available. In contrast, there is an established causal relationship between *T. vaginalis* infection and adverse pregnancy outcomes (9). Similarly, *T. vaginalis* infection was associated with low birth weight and preterm delivery in 40% of black women (57, 279). In that study, in which 14,000 American women were examined, *Trichomonas* was also associated with high infant mortality. In cattle, *Trichomonas foetus* infection causes infertility, which results in a tremendous economic loss (55, 133). It was suggested that *T. vaginalis* infection, as well as other STDs, increases susceptibility to HIV infection due to local inflammation and microscopic breaches in mucosal barriers (282). It was also suggested that *T. vaginalis* infection predisposes HIV carriers to symptomatic AIDS (211, 292). However, this issue is still debatable. Conversely, immunosuppression from HIV infection increases susceptibility to STDs (173, 211, 250, 282, 283, 292).

ENERGY METABOLISM OF "AMITOCHONDRIATE" PARASITES

Divergence of Mitochondrion-Related Organelles

Most higher eukaryotic organisms, including mammals, depend primarily on aerobic metabolism for their energy production. In contrast, certain anaerobic/microaerophilic eukaryotes, including *Entamoeba*, *Giardia*, and *Trichomonas*, lack typical and morphologically discernible mitochondria and the cytochrome-mediated oxidative phosphorylation found in aerobic organisms (217). Accordingly, these three parasites are often misleadingly referred to as "amitochondriate" protists. However, it is now well established that these organisms possess mitochondrion-related organelles, often with reductive or sometimes divergent functions (49, 104, 179, 194, 303, 304). For detailed discussions of the phylogenetic and biochemical aspects of the mitochondrion-related organelles, consult references 85, 86, 87, and 316. For the most recent reviews on the evolution of "amitochondriate" parasites, see references 84 and 156. These "amitochondriate" protists rely on substrate-level phosphorylation during glycolysis for ATP generation and mostly on fermentative metabolism for energy production (Fig. 1a and b). While the vestigial organelles or "mitosomes" (or "crypton" in *E. histolytica*) in *E. histolytica* and *G. intestinalis* retain only residual mitochondrial functions (49, 104, 194, 303, 304), the highly specialized mitochondrion-related organelle or "hydrogenosome" in *T. vaginalis* has compartmentalized pyruvate oxidation (168, 179, 215–219) (Fig. 2).

Besides compartmentalized energy metabolism in the *T. vaginalis* hydrogenosome, functional differences exist in the mitochondrion-related organelles among these three organisms. It was recently demonstrated that the ISC pathway, involved in iron-sulfur (Fe-S) cluster formation, is localized in the mitosomes of *G. intestinalis* and the hydrogenosomes of *T. vaginalis* (294, 304). In contrast, the *E. histolytica* mitosome lacks the ISC system. Instead, *E. histolytica* possesses a nitrogen fixation (NIF)-like system localized in the cytosol that is similar to that found in enteric *Epsilonprotobacteria* (15; V. Ali et al., unpublished data). Fe-S cluster biosynthesis is further described in "Physiological Importance of Cysteine and Fe-S Cluster Biosynthesis" below.

Diversity in the Conversion of Phosphoenolpyruvate to Acetyl Coenzyme A via Pyruvate

In *Entamoeba*, *Giardia*, and *Trichomonas*, glucose is not oxidized to CO_2 and H_2O as it is in aerobic metabolism but is instead catabolized to acetate, succinate, ethanol, alanine, and CO_2. The predominant metabolic end products and catabolic pathways depend on the organism and its environmental and physiological (e.g., drug sensitivity) states (see below). The pathways involved in the biosynthesis of pyruvate from phosphoenolpyruvate (PEP) diverge among these organisms (Fig. 1a). *G. intestinalis* can utilize three pathways to synthesize pyruvate: through pyruvate kinase (PK), pyruvate phosphate dikinase (PPDK), and a pathway mediated by PEP carboxyphosphotransferase, malate dehydrogenase (oxaloacetate to malate), and malic enzyme (decarboxylating, malate to pyruvate). It was assumed that, in *G. intestinalis*, the conversion of PEP to pyruvate operated mainly through PPDK (7). Although

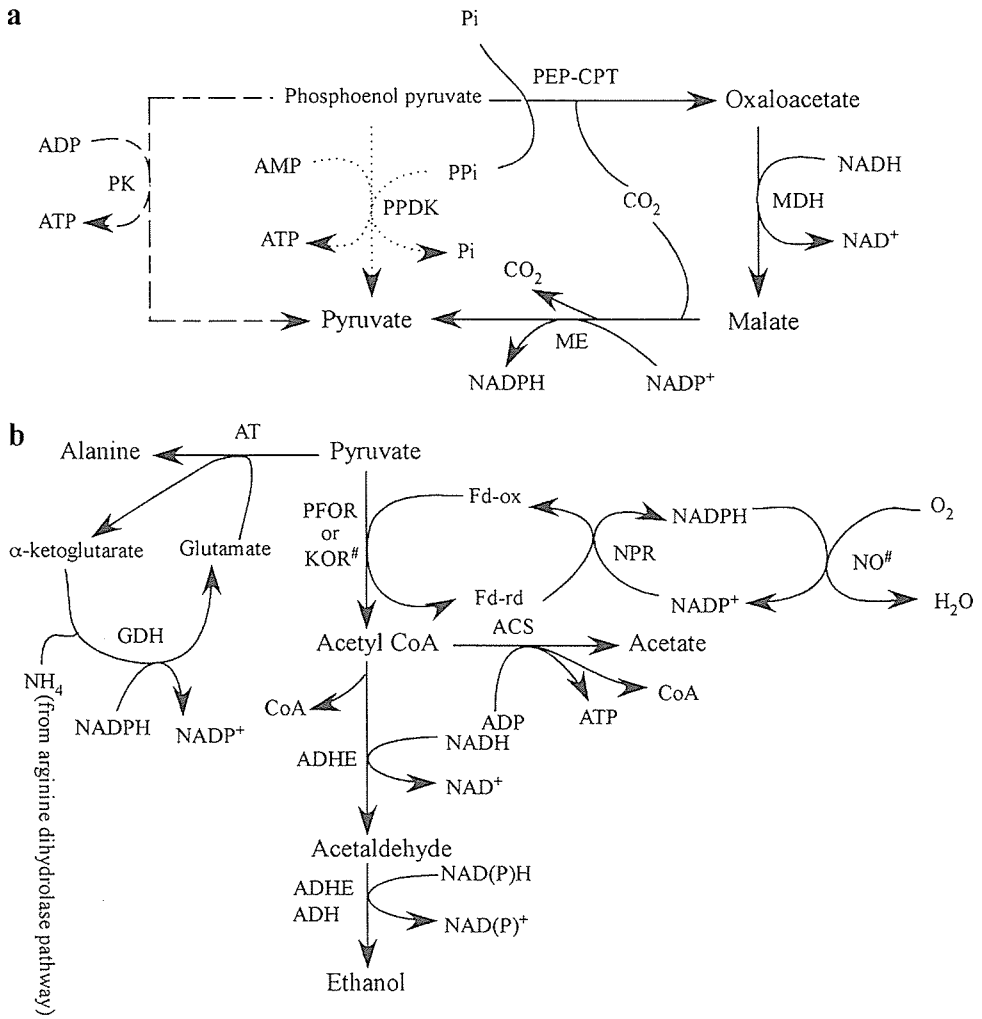

FIG. 1. Biosynthesis of pyruvate and its end products in "amitochondriate" protozoan parasites. (a) Synthesis of pyruvate from phosphoenolpyruvate in *G. intestinalis*, *E. histolytica*, and *T. vaginalis*. CPT, carboxyphosphotransferase; MDH, malate dehydrogenase (oxaloacetate to malate); ME, malic enzyme (decarboxylating, malate to pyruvate); Pi, inorganic phosphate; PPi, inorganic pyrophosphate. Solid arrows indicate a pathway that is optional in all three protists, while a pathway that generally plays a major role in the conversion of PEP to pyruvate is represented by dotted arrows for *E. histolytica* and *G. intestinalis* and by dashed arrows for *T. vaginalis*. (b) Metabolic pathways from pyruvate to its end products under anaerobic, microaerophilic, or aerobic conditions in *E. histolytica* and *G. intestinalis*. AT, alanine aminotransferase; GDH, glutamate dehydrogenase; KOR, 2-keto acid oxidoreductase; NO, NADH oxidase; ACS, acetyl-CoA synthase; ADHE, acetaldehyde/alcohol dehydrogenase (NAD dependent); ADH, alcohol dehydrogenase (NADP dependent); NPR, nitroperoxiredoxin or ferredoxin nitroreductase; Fd-ox, oxidized ferredoxin; Fd-rd, reduced ferredoxin. Acetate is the major product under aerobic conditions, while ethanol or alanine is preferentially produced under microaerophilic or strict anaerobic conditions, respectively. Note that ADHE is a fusion protein of acetaldehyde dehydrogenase and alcohol dehydrogenase. #, enzymes demonstrated only in *G. intestinalis*.

it was reported earlier that *E. histolytica* lacks PK activity (255) and that pyruvate is synthesized either by PPDK or through the third pathway mediated by PEP carboxyphosphotransferase, malate dehydrogenase, and malic enzyme, a recent report demonstrated the presence of PK activity and a putative PK gene in *E. histolytica* (269). No PPDK activity has been detected in *T. vaginalis* (209), and pyruvate is synthesized predominantly by PK or through the oxaloacetate/malate pathway. Although two PPDK genes were reported recently in *T. vaginalis* (288), functional characterization of these genes is lacking. The glycolytic pyrophosphate-dependent enzymes PPDK and phosphofructokinase are proposed targets for therapeutic intervention. These pyrophosphate-dependent enzymes are absent in the human host and can be inhibited with pyrophosphate analogues such as bisphosphonates. In order to validate PPDK as a rational drug target, it is essential to understand which pathway plays the major role in pyruvate formation in these protozoan parasites. In particular, mechanisms that control the expression of individual pathways depending upon substrate availability, oxygen tension, and other environmental factors are not well understood.

The conversion of pyruvate to acetyl coenzyme A (acetyl-CoA) is catalyzed by pyruvate:ferredoxin oxidoreductase (PFOR), which utilizes ferredoxin rather than NAD^+ as an electron acceptor in *E. histolytica* (257), *G. intestinalis* (307, 308), and *T. vaginalis* (330) in place of the pyruvate dehydrogenase complex found in aerobic bacteria and eukaryotes. Pyruvate dehydrogenase in the mitochondria of aerobic eu-

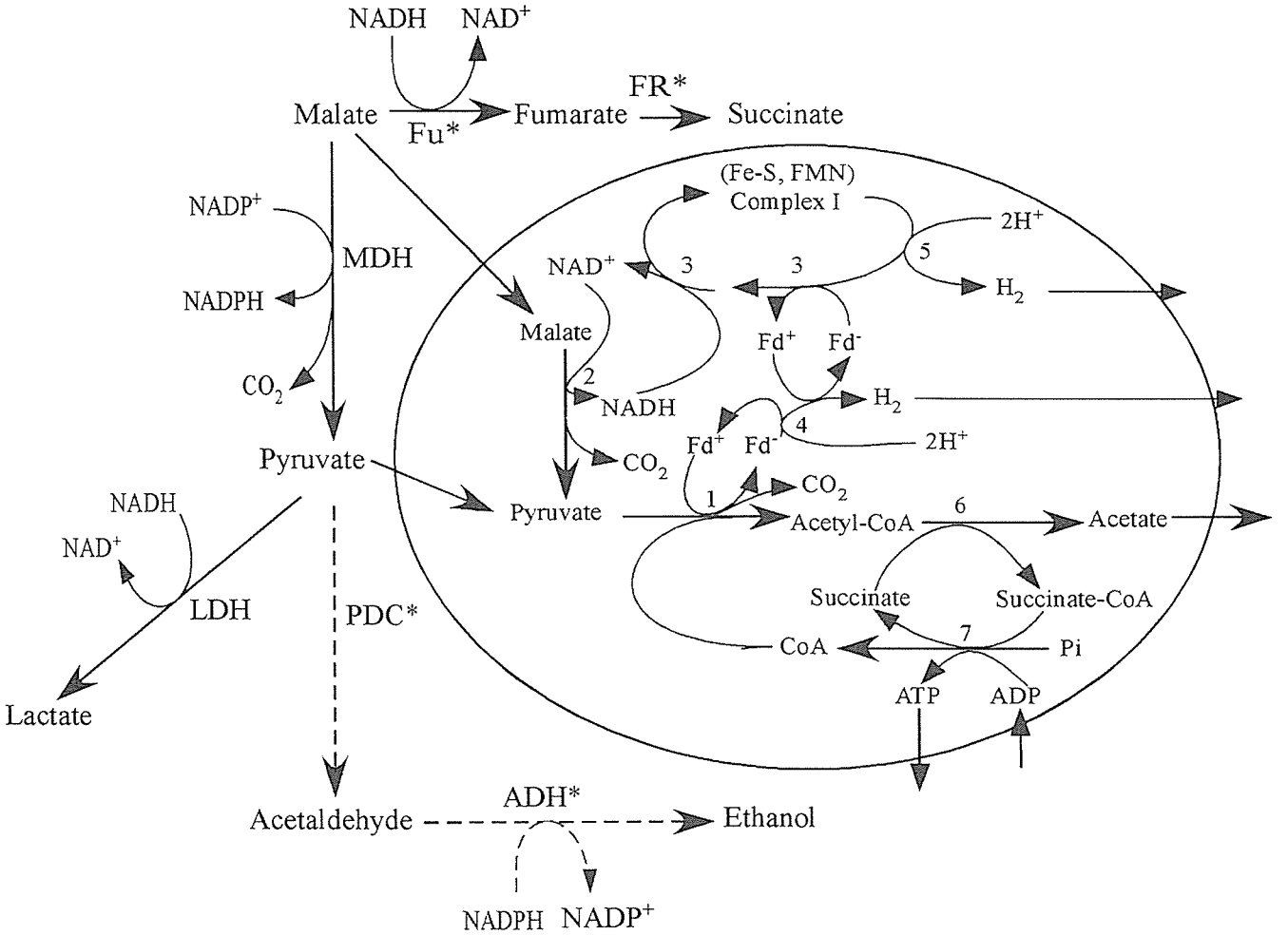

FIG. 2. Schematic map of pyruvate metabolism in the cytosol and the hydrogenosomes of metronidazole-sensitive and -resistant *T. vaginalis* and *T. foetus*. Enzymes marked with asterisks are demonstrated only in *T. foetus*. Steps depicted by dashed arrows were demonstrated only in metronidazole-resistant *T. foetus* strains. The major cytosolic end product in metronidazole-susceptible strains of *T. vaginalis* is lactate, and that in *T. foetus* is succinate. In metronidazole-resistant *T. vaginalis* or *T. foetus*, the major cytosolic end product is lactate or ethanol, respectively. LDH is not present in *T. foetus*. Acetate is produced only in hydrogenosomes of metronidazole-susceptible *T. vaginalis* and *T. foetus*. Abbreviations are as follows: MDH, malate dehydrogenase (decarboxylating, malate to pyruvate); LDH, lactate dehydrogenase; Fu, fumarase; FR, fumarate reductase; PDC, pyruvate decarboxylase; ADH, alcohol dehydrogenase; Fd-ox, oxidized ferredoxin; Fd-rd, reduced ferredoxin; Pi, inorganic phosphate. Steps indicated by numbers are catalyzed by the following enzymes: 1, pyruvate:ferredoxin oxidoreductase; 2, NADH-dependent malate dehydrogenase (decarboxylating); 3, NADH:ferredoxin oxidoreductase activity of 51-kDa and 24-kDa catalytic flavoprotein components of complex I; 4, ferredoxin-dependent Fe-hydrogenase; 5, hypothetical NADH-dependent 65-kDa Fe-hydrogenase; 6, acetate:succinate CoA-transferase; 7, succinate thiokinase.

karyotes catalyzes an oxidative decarboxylation to form acetyl-CoA and NADH. Energy metabolism in these protists was recently reviewed in more detail (112, 217).

Predominant End Products of Energy Metabolism

The end products of energy metabolism in "amitochondriate" protozoa are influenced by the O_2 tension (7). In addition, the major fermentation end products differ remarkably among these three organisms. For instance, in *G. intestinalis*, which has alanine aminotransferase, alanine is the major product of carbohydrate metabolism under strict anaerobic conditions (Fig. 1b) (243, 244). However, ethanol production is stimulated under conditions of low oxygen (<0.25 μM), while alanine production is suppressed; the major end products are ethanol and CO_2 (243). Under conditions of higher oxygen (>46 μM), where alanine production is completely inhibited, the major products from acetyl-CoA are acetate and CO_2. In contrast, the major end product in *E. histolytica* under anaerobic conditions is ethanol. A putative alanine aminotransferase gene is present in the *E. histolytica* genome, but its functional identity needs to be demonstrated (185). Under microaerophilic conditions, both ethanol and acetate are formed as end products (203, 325).

In *Trichomonas*, where part of the energy metabolism is compartmentalized in the hydrogenosome, electrons produced by the oxidation of pyruvate catalyzed by PFOR are donated to an Fe-hydrogenase via ferredoxin, which produces hydrogen gas (H_2) by transferring electrons to hydrogen ions (Fig. 2). ATP is generated exclusively by substrate-level phosphoryla-

tion in the hydrogenosomes (75). In wild-type *T. vaginalis*, the major end product from pyruvate is lactate produced by lactate dehydrogenase in the cytosol; lactate dehydrogenase is present only in *T. vaginalis*. The preferred end product also differs between *Trichomonas* species and between wild-type and drug-resistant strains (168) (see below). In metronidazole-susceptible *T. foetus*, a *Trichomonas* species that affects cattle, either succinate or ethanol is the major or minor metabolic end product, respectively, in the cytosol (168), because lactate dehydrogenase is absent in this organism. In the hydrogenosomes, acetate is the only end product of both metronidazole-susceptible *T. vaginalis* and *T. foetus* strains. In contrast, major end products in the cytosol of metronidazole-resistant *T. vaginalis* and *T. foetus* strains are lactate and ethanol, respectively.

Recently the NADH dehydrogenase module (also called NADH:ubiquinone oxidoreductase) of complex I was identified in *T. vaginalis* (75, 140, 141). Similar to mitochondrial respiratory complex I, NADH dehydrogenase can reduce a variety of electron carriers, including ubiquinone. Unlike the mitochondrial enzyme, ferredoxin is used as an electron carrier for hydrogen production in a reaction catalyzed by ferredoxin-dependent Fe-hydrogenase. Malate is one of the major hydrogenosomal substrates and is oxidatively decarboxylated to form pyruvate and CO_2 by a NAD-dependent malic enzyme. The electrons are transferred from NADH to ferredoxin by an NADH dehydrogenase homologous to the catalytic module of mitochondrial complex I. Thus, the discovery of an NADH dehydrogenase module of complex I solved the long-lasting conundrum of how *Trichomonas* regenerates NAD^+, which is essential for malate oxidation in the hydrogenosome (Fig. 2).

It was previously shown that *T. vaginalis* possesses two additional 2-keto acid oxidoreductases besides PFOR for energy production (34). These two 2-keto acid oxidoreductases, KOR1 and KOR2, prefer indolepyruvate as a substrate. KOR1 is present in both metronidazole-sensitive and -resistant strains, while KOR2 is present only in metronidazole-resistant strains of *T. vaginalis* (34, 73, 313). It was reported that 2-keto acid oxidoreductase activity increased in the metronidazole-resistant strain (34). However, neither KOR1 nor KOR2 could donate electrons to ferredoxin in the metronidazole-resistant line, because no detectable ferredoxin was produced in this strain (73) (see below).

Three Major Iron-Sulfur Proteins That Play an Essential Role in Energy Metabolism

Pyruvate:ferredoxin oxidoreductase. Eukaryotic PFOR is a homodimeric protein with a molecular mass of ~200 to 300 kDa containing 2[4Fe-4S] clusters and thiamine phosphate. Its structure is similar to that of PFORs from a wide range of eubacteria (138); e.g., PFOR from the eubacterium *Clostridium acetobutylicum* is a homodimer of 123-kDa subunits (207). PFOR from the thermophilic archaebacterium *Pyrococcus furiosus* is composed of four fragmented subunits (29, 161), all of which share significant homology to PFORs from eubacteria, fungi, and protists (138). PFORs from *E. histolytica*, *G. intestinalis*, and *T. vaginalis* are homodimers of 240 to 280 kDa containing 2[4Fe-4S] clusters and thiamine phosphate (257, 264, 308, 330). Despite the similar overall structure and the Fe-S clusters of PFORs in these "amitochondriate" protists, the intracellular localization of PFOR is divergent. While PFORs from both archaea and eubacteria are cytosolic, biochemical characterization (179, 330) has established that PFOR is localized to hydrogenosomes and is associated with the hydrogenosome membrane in *T. vaginalis* (330). In addition, a 120-kDa surface glycoprotein that shares cross-reacting epitopes with PFOR is involved in the adhesion of *T. vaginalis* trophozoites (213). This may suggest that PFOR or a PFOR-related protein is associated with hydrogenosomes and the plasma membrane, but this premise is still a matter of debate and needs to be independently verified. The PFORs from both *G. intestinalis* (81, 308) and *E. histolytica* (263, 274) were also suggested to be associated with the plasma membrane. PFOR was shown to be associated with the plasma membrane and with a cytoplasmic structure in *E. histolytica* that appeared as a ring form or a compact small body (263). However, the majority of PFOR activity was detected in an 80,000 × *g* supernatant fraction (257), suggesting that the proposed membrane association of *E. histolytica* PFOR (263, 274) might be transient and/or weak. At the primary sequence level, *T. vaginalis* PFOR possesses the putative mitochondrial targeting peptide at the amino terminus (142). In contrast, neither *E. histolytica* nor *G. intestinalis* PFOR possesses the mitochondrial targeting sequence. Since pyruvate metabolism is not compartmentalized in either of these organisms like it is in *T. vaginalis*, the physiological significance of the possible membrane association of PFOR in *G. intestinalis* and *E. histolytica* is not well understood.

Ferredoxin. Ferredoxin is another important class of proteins containing Fe-S clusters. Ferredoxins in the three microaerophilic/anaerobic parasitic protists differ in the nature of the Fe-S clusters they contain and their intracellular localization, i.e., cytosolic or hydrogenosomal. The *E. histolytica* genome encodes at least three ferredoxins (185), all of which contain either 2[4Fe-4S] clusters or [4Fe-4S] and [3Fe-4S] clusters, which correspond to a molecular mass of ~6 kDa, as previously characterized (256). *E. histolytica* apparently lacks [2Fe-2S] ferredoxin (15, 17), but ferredoxins containing these clusters are present in *T. vaginalis* and *G. intestinalis*. A larger ferredoxin from *Trichomonas* with one [2Fe-2S] cluster corresponding to a molecular mass of ~10 kDa was biochemically characterized and was localized in hydrogenosomes (116). The genome of *G. intestinalis* encodes at least four ferredoxins: one ferredoxin containing one [2Fe-2S] cluster (ferredoxin I) and three ferredoxins containing either 2[4Fe-4S] clusters or one [4Fe-4S] cluster and one [3Fe-4S] cluster (ferredoxins 1 to 3) (229). Among these ferredoxins, only ferredoxin I was shown to accept electrons from PFOR in vitro (308). The physiological role of [4Fe-4S] ferredoxins in *G. intestinalis* remains unclear. The small 2[4Fe-4S] ferredoxin of *E. histolytica* is evolutionarily closest to ferredoxin from anaerobic bacteria (143), while the larger [2Fe-2S] ferredoxin of *Trichomonas* hydrogenosomes shows a close kinship to ferredoxins of the cytochrome P450-linked mixed-function oxidase systems of bacterial and vertebrate mitochondria (154).

In addition, *G. intestinalis* possesses two genes, and *E. histolytica* possesses one gene, encoding a putative ferredoxin nitroreductase which consists of an amino-terminal 2[4Fe-4S] ferredoxin domain and a carboxyl-terminal nitroreductase domain (229). This ferredoxin-nitroreductase may be a physio-

logical acceptor of electrons from ferredoxin or PFOR and may be responsible for the activation of metronidazole. A ferredoxin-nitroreductase with a similar overall structure was also discovered in the whole-genome sequence of *Clostridium acetobutylicum* (231).

T. vaginalis ferredoxin possesses a [2Fe-2S] cluster and an 8-amino-acid putative mitochondrial targeting sequence at the amino terminus (154), similar to that of *G. intestinalis* [2Fe-2S] ferredoxin. Recently, the mitosome-targeting signal of *G. intestinalis* [2Fe-2S] ferredoxin was shown to target ferredoxin to the hydrogenosome of *T. vaginalis*, suggesting that the mitosome and the hydrogenosome share a common mode of protein targeting similar to the protein import machinery of mitochondria (69). Similarly, the mitochondrial targeting signal from *Trypanosoma cruzi* was also shown to be interchangeable with that of *E. histolytica* (303, 316). While import of ferredoxin and IscU, a scaffolding protein for iron-sulfur biosynthesis, relies on the amino-terminal signal, the targeting of other mitosomal proteins (e.g., the catalytic component of iron-sulfur cluster biosynthesis IscS, Cpn60, and mitochondrial Hsp70) into the mitosome does not require this presequence in *G. intestinalis* (258). The underlying mechanisms of mitosome import of the latter proteins are not clear, but they likely possess cryptic internal signals, as demonstrated in the ADP-ATP carrier protein localized in the hydrogenosome of *T. vaginalis* (74) and other proteins found in the inner membrane of mitochondria (248). Mitosome import of Cpn60 relies on the presequence in *E. histolytica* (303), suggesting organism dependence in the targeting mechanisms. It also remains to be determined which ferredoxin(s) among the three types is involved in energy metabolism and redox regulation as well as the activation of metronidazole in *E. histolytica* and *G. intestinalis*. It is also unknown why different types of ferredoxins are retained throughout the evolution of these parasites.

Hydrogenase. Hydrogenases are enzymes responsible for producing hydrogen gas by transferring electrons to two protons. Hydrogenases are oxygen sensitive and are present in a wide range of anaerobic bacteria and hydrogenosomes from certain microaerophilic/anaerobic protozoan parasites, ciliates, fungi, and chytrids (86, 87, 136, 251). Two types of hydrogenases are known; heterodimeric NiFe-hydrogenase and monomeric Fe-hydrogenase. The heteromeric NiFe-hydrogenases consist of a large subunit containing a bimetalic NiFe cluster at the hydrogen-activating site and a small subunit containing up to three Fe-S clusters that transport electrons to the physiological acceptors. NiFe-hydrogenases are generally involved in H_2 uptake in archaebacteria and eubacteria (46). In contrast, the mostly monomeric Fe-hydrogenases usually catalyze H_2 evolution (98). In some bacteria, e.g., the hyperthermophilic bacterium *Thermotoga martima* and the anaerobic bacterium *Desulfovibrio fructosovorans*, Fe-hydrogenase is composed of two or three subunits sharing homology with monomeric Fe-hydrogenases (113, 318). *T. vaginalis* possesses at least three Fe-hydrogenase genes (42, 137). There are two types of Fe-hydrogenases, referred as "short-form" (50-kDa) and "long-form" (64-kDa) Fe-hydrogenases (86). These Fe-hydrogenases, which differ in size due to the heterogeneity at the amino-terminal end, have been well studied (42, 137). An overlapping region of 450 amino acids of the longer *T. vaginalis* form of Fe-hydrogenases showed 47% amino acid identity to short-form Fe-hydrogenases (137). While the 50-kDa Fe-hydrogenase contains 2[4Fe-4S] clusters and lacks the mitochondrion/hydrogenosome-targeting sequence, the 64-kDa Fe-hydrogenase possesses an amino-terminal extension containing additional [4Fe-4S] and [2Fe-2S] clusters and the mitochondrion-targeting signal (137), suggesting that long-form Fe-hydrogenase is fully active and accepts electrons from ferredoxin (86).

An Fe-hydrogenase gene was also identified in *G. intestinalis* and *E. histolytica* (137, 228), and its enzymatic activity and/or mRNA expression was demonstrated in cultured *E. histolytica* and *G. intestinalis* (228). However, a recent report suggests that *Giardia* produces hydrogen at a 10-fold-lower rate than *T. vaginalis* does (183). The physiological role of Fe-hydrogenase in *E. histolytica* and *G. intestinalis* has not been clearly demonstrated as in *T. vaginalis*, where hydrogenase plays an indispensable role in the final transfer of electrons to protons (218). Recently, auxiliary Fe-hydrogenase maturases (*S*-adenosylmethionine-dependent HydG, HydE, and the small GTPase HydF) were identified from the *T. vaginalis* hydrogenosomes by proteomic analysis and from the genome database (251), which further elucidates the molecular mechanisms of biosynthesis and maturation of Fe-hydrogenase in this parasite.

CURRENT CHEMOTHERAPEUTICS

Current Chemotherapeutics for *E. histolytica* Infection

Since emetine was first shown to be effective against *E. histolytica* infection in 1912 (162), the present antiamoebic drugs that are most commonly used are 5-nitroimidazoles, including metronidazole (Flagyl) and tinidazole (Fasigyn). For years, these two drugs have proven to be effective against invasive intestinal and extraintestinal amoebiasis. Although metronidazole is considered the drug of choice (286), nitroimidazoles with longer half-lives such as tinidazole and ornidazole allow for a single dose, better tolerance, and shorter treatment time. Metronidazole (750 mg) and tinidazole (800 mg) three times a day are generally used for 7 and 5 days, respectively. Alternatively, a single dose (2 g) of tinidazole or ornidazole is generally recommended for treatment of amoebiasis or giardiasis. In addition, chloroquine, emetine, and dehydroemetine are used for cases that do not respond to metronidazole or tinidazole alone (26, 286). Since all of these compounds are well absorbed in the intestine, they are generally ineffective for asymptomatic cyst passers. To treat cyst carriers with 5-nitroimidazoles, the course of treatment is generally extended for a minimum of 10 days, which produces some success. Patients occasionally suffer from a relapse of invasive amoebiasis months after a short course of metronidazole therapy (26, 286). A single high-dose therapy with 2 g metronidazole is preferred over therapy with multiple doses or over an extended period, but it is not tolerated in some patients, including pregnant women and alcoholics. Lumen-acting drugs, such as diloxanide furoate (Furamide) (500 mg three times a day for 10 days), iodoquinol (Yodoxin) (650 mg three times a day for 20 days), and paromomycin (Humatin) (25 to 35 mg in three doses for 7 days), have been used to eliminate dormant luminal cysts and prevent relapses. However, asymptomatic cases that fail to respond to this extended therapy are occasionally ob-